

Chromatic Dispersion Estimation Based on Signal Power Distribution

Meng Qiu, Xuefeng Tang, Chunpo Pan, Qingyi Guo, Wing-Chau Ng, Tianyu Zhao, and Chuandong Li

Huawei Technologies Canada Co., Ltd., Ottawa, Canada, K2K 3J1, meng.qiu@huawei.com

Abstract *We propose two new cost functions for the best-match search in a chromatic dispersion (CD) estimator based on the power distribution of the time-domain signal samples. They can supplement the conventional peak-to-average power ratio (PAPR) based metric to achieve more robust CD estimation.*
©2023 The Author(s)

Introduction

In coherent optical communication systems, chromatic dispersion (CD) can be compensated effectively in digital domain as part of the receiver-side digital signal processing (DSP). The amount of the accumulated CD can be estimated using various methods [1-8]. Some of these methods rely on a “best-match search” process, i.e., they calculate certain cost functions after applying different test CDs to the signal, and these cost functions are expected to show a maximum or minimum value when the test CD matches the actual one. Although these best-match-search-based methods seem time-consuming, they are generally robust and more implementable [2]. Specifically, the author of [6] proposed to use the peak-to-average power ratio (PAPR) of the test-CD-compensated signal as the cost function, which is simple and works well under various system conditions. However, this approach is less effective for signals with probabilistic constellation shaping (PCS). One explanation is that the PAPR of the non-dispersed waveform tends to increase in the scenarios with PCS, meaning that its difference relative to the PAPR of the dispersed signal becomes less significant, as shown in Fig. 1(a).

In this paper, we propose two new cost functions for the best-match search of the CD estimation (CDE), which, similar to the PAPR based approach, work on the time-domain (TD) signal samples. Our objective is to extract more information from the signal’s sample power distribution while the conventional PAPR based method merely focuses on the peak power. As a result, the estimator’s robustness is expected to be improved.

Principle

In coherent optical communication systems, sufficient amount of CD makes the amplitude distribution of each TD signal tributary close to a Gaussian distribution. One such example is illustrated in Fig. 1(b), where X_I represents the in-phase component of the X-polarization. In this

example, CD is the only system impairment added to a 90-Gbaud, root-raised-cosine (RRC) pulse-shaped 16-QAM signal. The roll-off factor of the pulse shaping is 0.2, and the over-sampling rate of 1.25. Correspondingly, if we assume there are no impairments causing correlation or imbalance between signal tributaries, the power of the dual-polarization complex samples p_n should follow a Chi-square distribution with 4 degrees of freedom, as shown in Fig. 1(c). In this work, we will call such power distribution the “hypothesized power distribution (HPD)”, and it happens when sufficient amount of CD is applied to the signal. On the other hand, we call the sample power distribution at zero CD the “intrinsic power distribution (IPD)”. It is related to the signal pattern itself as well as the system configurations other than CD, and it is typically different from the HPD. It is noted that although we start from the assumption of an “ideal” system while in practice various system impairments will smear the gap between the HPD and the IPD, we found that some distribution differences may still be observable with practical types and amounts of impairments, as shown in Fig. 1(c). Therefore, we can define a divergence term representing the difference between the HPD and the sample power distribution under a specific test CD (PDuT). Then during the best-match search, this divergence term is supposed to be the most significant when the PDuT is the closest to the IPD, or equivalently, the test CD is the best match of the actual CD. In this work, we elaborate two specific proposals motivated by this idea. These new metrics can further be combined with the PAPR term to construct the cost function, and the diagram of one such example is shown in Fig. 2.

In the first proposal, we define the divergence term based on the number of “small-power samples”, as in Fig. 1(c) we observe the probability density of the IPD is lower than the HPD in the low-power region. Specifically, we will count the number of samples whose power is smaller than a pre-defined threshold p_{th} , i.e., $\text{count}\{p_n < p_{th}\}$, and p_{th} can be optimized based

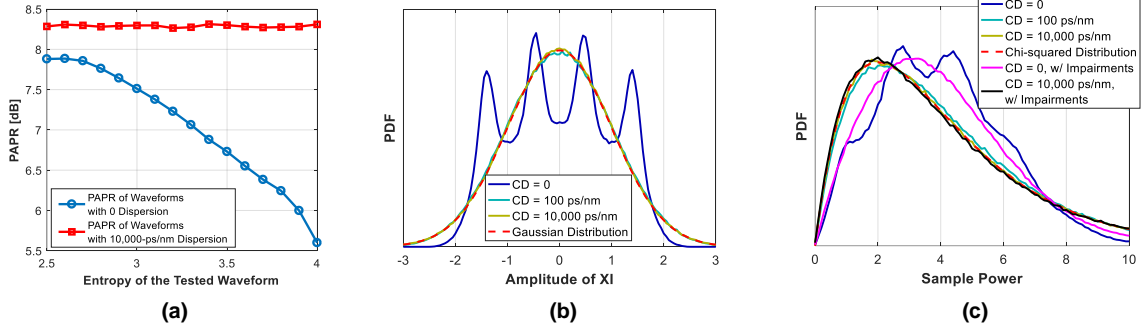


Fig. 1: (a) PAPR of different tested PCS-16-QAM waveforms; (b) an example of the amplitude distribution of the XI samples with different amounts of CD; (c) an example of the power distribution of the dual-polarization complex samples with different amounts of CD.

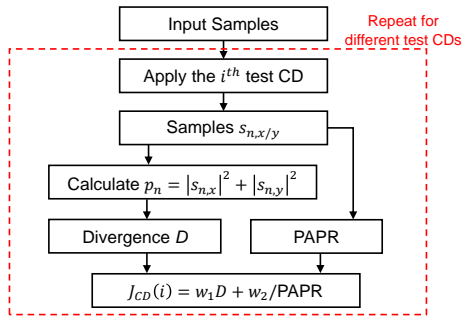


Fig. 2: One example of combining the proposed metrics with PAPR. w_1 and w_2 represent the weights of the two terms.

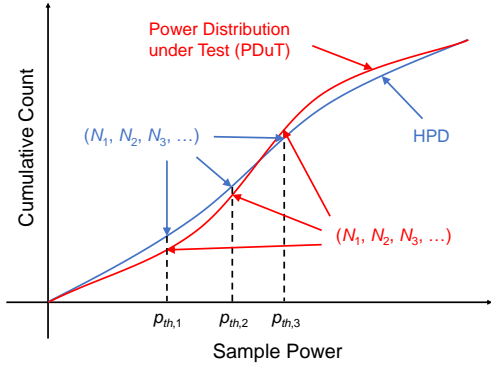


Fig. 3: Approximation of a distribution's CDF.

on the actual sample power distributions. Finally, the divergence term is defined as $D = 1/\text{count}\{p_n < p_{th}\}$.

In the second proposal, we evaluate the goodness of fit between the HPD and the PDuT. Specifically, we first obtain a distribution's empirical cumulative distribution function (CDF) based on K bins, as shown in Fig. 3. Ignoring some re-scaling factors, this process is similar to counting the number of samples with power smaller than a threshold (as in the first proposal), but now we will define multiple thresholds with appropriate spacing as $(p_{th,1}, p_{th,2}, \dots, p_{th,K})$. Next, we obtain a vector of "counts" as $\vec{N} = (N_1, N_2, \dots, N_K)$, where $N_k = \text{count}\{p_n < p_{th,k}\}$, $k = 1, 2, \dots, K$. The divergence term is then calculated as [9]

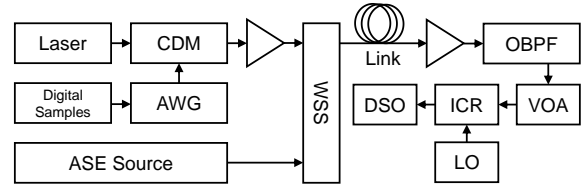


Fig. 4: Experimental setup. CDM: coherent driver modulator; VOA: variable optical attenuator; LO: local oscillator.

$$D = \sum_{k=1}^K \frac{(N_{PDuT,k} - N_{HPD,k})^2}{N_{HPD,k}(N_{total} - N_{HPD,k})} (N_{HPD,k} - N_{HPD,k-1})$$

where the subscripts "PDuT" and "HPD" mean the counts are for the PDuT and for the HPD respectively, N_{total} is the total number of samples, and $N_{HPD,0}$ is 0. Note that to obtain the HPD, we need to generate a reference signal that carries a sufficient amount of CD, and this can be realized by applying an "unrealistic CD" to the test signal. Simulation (not shown here) indicates that satisfactory results can be achieved with $K < 10$, meaning that this second proposal can also be implemented with reasonable complexity.

It is noted that essentially the PAPR based metric also utilizes the signal power distribution, but it only focuses on the high-power range. On the other hand, in our proposals, we extract more information from the low-power range or even the entire distribution.

Experiment

The system for a proof-of-concept experiment is outlined in Fig. 4. The symbol rate was 90 Gbaud. The single-carrier signals under test had different entropies with a 16-QAM base constellation, and the entropies here were simply calculated based on the symbol probabilities. To construct the transmitted waveforms, the symbols were first generated offline block-wise, and each block of 128 symbols had constant composition of symbol magnitudes. The only exception was the test case with an entropy of 4 where each symbol was generated independently. After up-sampling and

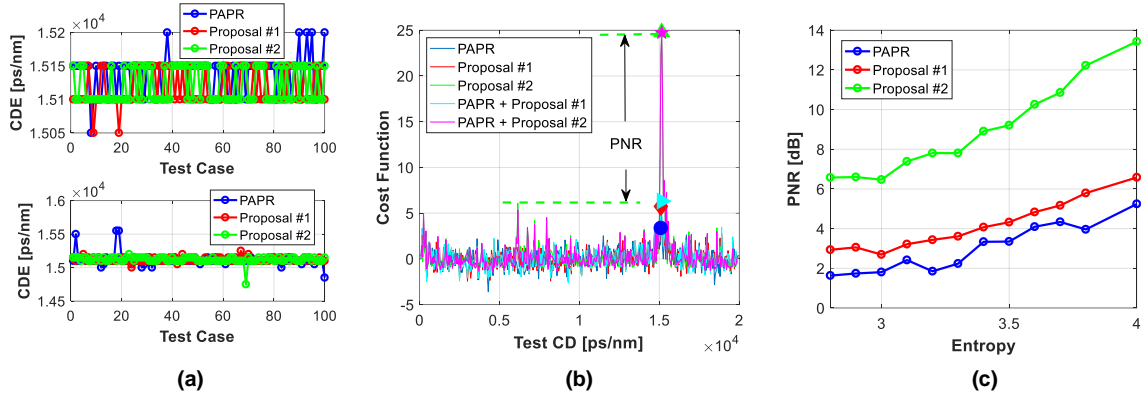


Fig. 5: (a) CDE when the tested waveform has entropy of 3.5 (top) and 2.8 (bottom); (b) an example of the cost function curves of different methods when the entropy of the tested waveform is 2.8; (c) averaged PNR vs the entropy of the tested waveforms using different methods.

RRC pulse shaping, the digital samples were uploaded to an arbitrary waveform generator (AWG) and further modulated to the optical signal. This test channel was then combined with an amplified spontaneous emission (ASE) source which contained two 400-GHz noise bands, and the test channel was located in the middle of the 200-GHz gap between the two noise bands. The wavelength selective switch (WSS) was configured to make the test channel and the ASE bands have similar power spectral density. Afterwards, the combined signal was launched to a 12-span link, and each span consisted of ~75 km of standard single mode fiber and an optical amplifier. The launched power to the link was optimized based on the overall system performance. At the receiver, the test channel was selected by a 100-GHz optical bandpass filter (OBPF) before it was detected by an integrated coherent receiver (ICR). A digital storage oscilloscope (DSO) then captured 4 million samples for each signal tributary at 160 GS/s. Finally, the received digital samples were down-sampled and processed by different CDE methods.

Based on the system parameters, we chose a CD scan range of 0 – 20,000 ps/nm and a scan step of 50 ps/nm. To emulate the real-time data flow in a practical system, we used a randomly located window to select 64,000 samples out of the entire captured sequence for each test CD, and this avoids using identical data patterns repeatedly. Afterwards, the middle 48,000 samples were used for cost function calculation. In the PAPR based method, the PAPR term was calculated every 480 samples, and these numbers were then averaged before serving as the cost function.

From the experiment results in Fig. 5(a), we observe that all the methods provide a CDE of around ~15,100 ps/nm when the entropy of the tested signal is 3.5. These CDE values are

reasonable as they match the link parameters. However, all the methods tend to be less effective when the entropy decreases to 2.8 and even return incorrect results occasionally. For further comparison of different methods, we take the reciprocal of the PAPR term so that the corresponding cost function curve shows a peak at the correct CD. Then we offset the cost functions of all the methods such that the “noise floors” of the curves have zero mean. After these manipulations, we define a metric called peak-to-noise ratio (PNR) by comparing the magnitudes between the peak of the cost function curve and the most significant interferer. Fig. 5(b) illustrates the PNR definition with a specific example. The PNRs of different methods averaged over 100 test cases are summarized in Fig. 5(c). Statistically, both proposals outperform the PAPR based method over the entire entropy range under test. A specific test case is also studied in depth in Fig. 5(b). For an easier comparison, all cost function curves are re-scaled such that their noise floors have similar root mean square (RMS) values, and the peaks of the curves are highlighted by markers. It is observed that the cost function curve of the PAPR based method only shows a weak peak at the correct CD. In contrast, the peaks of the proposed cost functions are stronger (although some interferers may also get enhanced at the same time). In addition, combining the proposed metrics with PAPR also leads to slightly improved PNR in this specific test case.

Conclusions

We propose two new cost functions for the best-match search in a CD estimator by extracting information other than PAPR from the signal power distribution. Their effectiveness has been verified experimentally.

References

- [1] L. Cheng, Z. Li, C. Lu, A. P. T. Lau, H. Y. Tam, and P. K. A. Wai, "Chromatic dispersion monitoring based on variance of received optical power," *IEEE Photonics Technology Letters*, vol. 23, no. 8, pp. 486-488, 2011, DOI: [10.1109/LPT.2011.2109944](https://doi.org/10.1109/LPT.2011.2109944).
- [2] R. Andres Soriano, F. N. Hauske, N. Guerrero Gonzalez, Z. Zhang, Y. Ye, and I. Tafur Monroy, "Chromatic dispersion estimation in digital coherent receivers," *Journal of Lightwave Technology*, vol. 29, no. 11, pp. 1627-1637, 2011, DOI: [10.1109/JLT.2011.2145357](https://doi.org/10.1109/JLT.2011.2145357).
- [3] C. Malouin, P. Thomas, B. Zhang, J. O'Neil, and T. Schmidt, "Natural expression of the best-match search Godard clock-tone algorithm for blind chromatic dispersion estimation in digital coherent receivers," in *Advanced Photonics Congress*, 2012, paper SpTh2B.4.
- [4] Q. Sui, A. P. T. Lau and C. Lu, "Fast and robust blind chromatic dispersion estimation using auto-correlation of signal power waveform for digital coherent systems," *Journal of Lightwave Technology*, vol. 31, no. 2, pp. 306-312, 2013, DOI: [10.1109/JLT.2012.2231400](https://doi.org/10.1109/JLT.2012.2231400).
- [5] C. Malouin, M. Arabaci, P. Thomas, Bo Zhang, T. Schmidt, and R. Marroccia, "Efficient, non-data-aided chromatic dispersion estimation via generalized, FFT-based sweep," in *Optical Fiber Communication Conference and Exposition and the National Fiber Optic Engineers Conference (OFC/NFOEC)*, Anaheim, CA, 2013, pp. 1-3, DOI: [10.1364/NFOEC.2013.JW2A.45](https://doi.org/10.1364/NFOEC.2013.JW2A.45).
- [6] C. Xie, "Chromatic dispersion estimation for single-carrier coherent optical communications," *IEEE Photonics Technology Letters*, vol. 25, no. 10, pp. 992-995, 2013, DOI: [10.1109/LPT.2013.2257729](https://doi.org/10.1109/LPT.2013.2257729).
- [7] H. Zhou, B. Li, M. Tang, K. Zhong, Z. Feng, J. Cheng, A. P. T. Lau, C. Lu, S. Fu, P. P. Shum, and D. Liu, "Fractional Fourier transformation-based blind chromatic dispersion estimation for coherent optical communications," *Journal of Lightwave Technology*, vol. 34, no. 10, pp. 2371-2380, 2016, DOI: [10.1109/JLT.2016.2538467](https://doi.org/10.1109/JLT.2016.2538467).
- [8] Y. Chen, Q. Sui, Z. Li, Z. Liang, and W. Liu, "Joint CD and PMD monitoring based on a pair of low-bandwidth coherent receivers," *Optics Express*, vol. 24, no. 23, pp. 26756-26765, 2016, DOI: [10.1364/OE.24.026756](https://doi.org/10.1364/OE.24.026756).
- [9] T. W. Anderson and D. A. Darling, "A test of goodness of fit," *Journal of the American Statistical Association*, vol. 49, no. 268, pp. 765-769, 1954, DOI: [10.2307/2281537](https://doi.org/10.2307/2281537).